

A Memory-Efficient, Adaptive Algorithm for Multipole-Accelerated Capacitance Computation in a Stratified Dielectric Medium

Vikram Jandhyala, Eric Michielssen, and Raj Mittra

Electromagnetic Communication Laboratory, Department of Electrical and Computer Engineering, University of Illinois, Urbana, Illinois 61801. E-mail: vikram@decwa.ece.uiuc.edu

Received June 12, 1995; revised December 21, 1995.

ABSTRACT

An adaptive, multipole-accelerated technique is presented for the fast computation of capacitances of conducting structures that reside in stratified dielectric media. This technique is an extension of a previously reported method of moments based approach that uses a nonadaptive fast-multipole algorithm in conjunction with a closed-form Green's function for a stratified medium. In the proposed adaptive technique, the specific spatial arrangement of the images introduced by this Green's function is exploited to significantly reduce the excessive memory requirements associated with the earlier technique. It is shown that the reduction in memory is attained in such a manner that both speed and accuracy are not adversely affected. © 1996 John Wiley & Sons, Inc.

1. INTRODUCTION

The computation of the capacitance matrices of conducting structures embedded in stratified dielectric media is critical for accurately modeling interconnect structures and for ensuring the proper functioning of electronic packages. Oh et al. [1] have characterized capacitances of microstrip bends and crossovers using the method of moments (MoM) in conjunction with a closed-form approximation to the Green's function for stratified dielectric media. The fast-multipole method (FMM) [2–6], a recently developed algorithm for efficient evaluation of the potential due to a given distribution of charges, has been employed in conjunction with the MoM to solve capacitance problems involving conductors residing in a homogeneous medium [7–10], and in the presence of finite-sized dielectrics [11, 12]. The latter studies utilize the expansion of the static potential in terms of a free-space Green's func-

tion in conjunction with an equivalent-charge formulation for the dielectric interfaces [13]. The fast computation of capacitances of conducting structures embedded in a layered dielectric medium is essential to the design of VLSI circuits. This problem was addressed by the authors in refs. 14 and 15, where the FMM was utilized to compute the capacitances of conductors residing in a stratified dielectric medium, by incorporating a closed-form approximation to the stratified medium Green's function [1] into the FMM framework. It was demonstrated that this technique is capable of solving capacitance problems involving layered media with considerably more numerical efficiency than non-FMM-based methods, whether they be direct or iterative, with little or no compromise in accuracy. The major drawback of the FMM-based algorithm for stratified media, introduced in ref. 14, over its free-space counterpart [7–12] is its large memory requirement, which is discussed in section 3. In this

follow-up communication, an adaptive algorithm is presented that significantly reduces the memory requirements over those of the nonadaptive, FMM-based algorithm presented in ref. 14. This reduction in memory is achieved by exploiting the spatial distribution of images relative to the positions of the conductors in the computational domain of the FMM. The proposed adaptive FMM-based algorithm produces capacitance matrix entries that are as accurate as those produced by the nonadaptive technique, and also does not require any more CPU time than that required by the earlier nonadaptive algorithm.

This communication is organized as follows. Section 2 presents an MoM-based technique for computing capacitances of conductors that reside in a stratified dielectric medium, and summarizes the nonadaptive FMM-based technique of ref. 14. Section 3 outlines the proposed adaptive algorithm and discusses its advantages over the nonadaptive algorithm [14] in terms of memory requirements. Numerical results are presented in section 4, and section 5 contains conclusions and suggestions for future work.

2. FORMULATION

Let n conductors reside in a stratified dielectric medium. We seek the $n \times n$ capacitance matrix, \mathbf{C} , of this system, which satisfies:

$$\mathbf{q} = \mathbf{C}\mathbf{p} \quad (1)$$

where \mathbf{q} and \mathbf{p} are column vectors of length n containing the total charge on each of the conductors, and the potential of each of the conductors, respectively. To compute \mathbf{C} , an integral equation is constructed in terms of the unknown charge density, $\sigma(\mathbf{r})$, residing on each conductor surface:

$$\psi^i(\mathbf{r}) = \int_S G(\mathbf{r}|\mathbf{r}')\sigma(\mathbf{r}') ds' \quad (2)$$

where S is the conductor surface, $\psi^i(\mathbf{r})$ is the known and impressed potential on S , and $G(\mathbf{r}|\mathbf{r}')$ is the spatial Green's function for potential evaluation in a stratified medium. $\sigma(\mathbf{r})$ is solved for by invoking the MoM [8]. To this end, the conductor surfaces are discretized into triangular patches, and compactly supported basis functions (typically pulse basis functions) are utilized to expand the unknown charge density $\sigma(\mathbf{r})$. Point matching the

resulting equations at the centers of the patches leads to a dense matrix equation relating \mathbf{V} , the vector of impressed potentials on the patches, to \mathbf{I} , the vector of expansion coefficients of the basis functions:

$$\mathbf{V} = \mathbf{Z}\mathbf{I} \quad (3)$$

The MoM matrix, \mathbf{Z} , is of dimensions $M \times M$, where M is the total number of patches. Eq. (3) may be solved, either directly or iteratively, to yield different columns of the capacitance matrix. These columns are obtained by setting the impressed potentials on the patches of a particular conductor to unity and all others to zero, and then summing up the resulting charges on patches on the surface of each conductor.

It has been demonstrated in ref. 14, that the use of the closed-form approximation, $G_{cf}(\mathbf{r}|\mathbf{r}')$, of the Green's function, $G(\mathbf{r}|\mathbf{r}')$, in a manner outlined in ref. 1, considerably simplifies the numerical evaluation of the MoM matrix elements. $G_{cf}(\mathbf{r}|\mathbf{r}')$ represents the potential due to a charge residing in a stratified dielectric medium in terms of the potential due to the genuine charge and a finite number of images, all residing in a homogeneous medium, as shown in Figure 1.

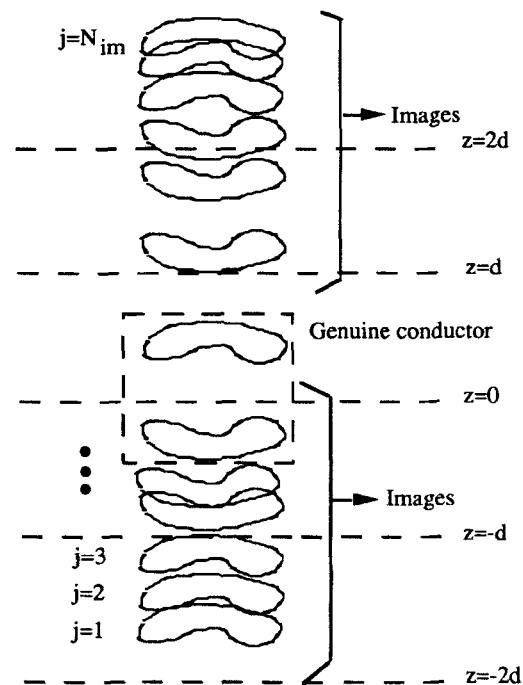


Figure 1. Images obtained from the use of the closed-form Green's function for multilayered dielectric media. The genuine conductor is embedded in a dielectric slab located in between $z = 0$ and $z = d$.

If an iterative method, such as GMRES [17], or the conjugate gradient method [18], is used to solve Eq. (3), evaluations of the matrix-vector product, $\mathbf{Z}\mathbf{I}_q$, where \mathbf{I}_q is a vector of trial coefficients associated with the charge distribution on the patches, are required. The product $\mathbf{Z}\mathbf{I}_q$ generates the potentials at the centers of the genuine patches due to charges on all the patches corresponding to the trial charge coefficient vector \mathbf{I}_q . Using $G_{cf}(\mathbf{r}|\mathbf{r}')$, defined in ref. 14, this evaluation is performed in the following manner:

$$\mathbf{Z}\mathbf{I}_q = \mathbf{Z}^s \mathbf{I}_q + \sum_{j=1}^{N_{im}} \mathbf{Z}_j^{im} k_j \mathbf{I}_q \quad (4)$$

where \mathbf{Z}^s is the MoM matrix for a homogeneous medium, and \mathbf{Z}_j^{im} is the contribution due to patches that correspond to the j th image. The charge coefficients on the image patches are dependent on \mathbf{I}_q and appear in eq. (4) as terms of the form $k_j \mathbf{I}_q$.

The direct evaluation of the matrix-vector product in eq. (4) entails $O(M^2)$ operations per iteration. The FMM may be invoked to evaluate the matrix-vector product in eq. (4) in an extremely efficient manner, requiring only $O(M)$ operations per iteration, as shown in ref. 14. Anderson's FMM technique [6], which is based on the use of Poisson's formula to represent the solution of Laplace's equation, is used here and in ref. 14. To facilitate the evaluation of the matrix-vector product in eq. (4), the entire multi-conductor structure, and all of the image patches, are enclosed in a large cubical volume, which is recursively partitioned into eight smaller cubes. For each cube at every level, an outer sphere approximation is conducted. Consider a sphere that encloses the cube and whose center coincides with that of the cube. Given the potential $g(\cdot)$ on the surface of this sphere S due to all the sources residing in the cube, the outer sphere formula:

$$\Psi(\mathbf{r}) = \frac{1}{4\pi} \int_S \left[\sum_{n=0}^{\infty} (2n+1) \left(\frac{h_o}{r_o} \right)^{n+1} P_n(\mathbf{s} \cdot \mathbf{r}_p) \right] \times g(h_o \mathbf{s}) ds \quad (5)$$

enables the computation of the potential $\Psi(\mathbf{r})$ at any observation point \mathbf{r} located outside S , where \mathbf{r}_p is the unit vector pointing from the center of the sphere toward \mathbf{r} , h_o is the radius of the sphere, r_o is the distance from the center of the

sphere to the point \mathbf{r} and $P_n(\cdot)$ is the n th Legendre function. Outer spheres approximations for progressively larger cubes are obtained by repeated use of eq. (5).

To evaluate the matrix-vector product in eq. (4), observation points are aggregated in a manner similar to that which is employed to aggregate source points. However, the observation points correspond to the centers of the genuine patches only, whereas both the genuine and the image patches comprise the sources. Consider a sphere with surface S that encloses a cube and whose center is the same as that of the cube. The potential, $\Psi(\mathbf{r})$, at any point, \mathbf{r} , inside this inner sphere, S , due to sources outside it, can be expressed as:

$$\Psi(\mathbf{r}) = \frac{1}{4\pi} \int_S \left[\sum_{n=0}^{\infty} (2n+1) \left(\frac{r_i}{h_i} \right)^n P_n(\mathbf{s} \cdot \mathbf{r}_p) \right] \times g(h_i \mathbf{s}) ds \quad (6)$$

where $g(\cdot)$ is the potential on the surface of the sphere S due to all sources outside it. At each level, the inner sphere approximation for every cube is constructed by considering the inner sphere approximation for the parent cube and adding to that the potentials due to outer spheres from those cubes that are well-separated and have not been accounted for in the construction of the inner sphere of the parent cube [6]. Eqs. (5) and (6) are approximated numerically by retaining a finite number of spherical harmonics, and utilizing nonproduct integration rules [19, 20], as done in Anderson [6] and Jandhyala et al. [14].

3. THE ADAPTIVE ALGORITHM

The nonadaptive fast multipole algorithm, discussed in the previous section, further termed FMM, computes the potentials at the centers of the genuine patches due to the charges on the genuine patches and the equivalent charges on the image patches. The overall memory requirement of FMM is in effect determined only by the number of outer and inner spheres that need to be stored. The remaining memory usage due to the storage of interactions between patches in cubes that are not well separated is negligible. Moreover, for the FMM algorithm described in ref. 14, the number of outer spheres typically far exceeds the number of inner spheres. This is because outer spheres are constructed for all

cubes that contain genuine and/or image patches, while inner spheres are constructed only for those cubes that contain genuine patches. In fact, in a worst-case scenario, the number of outer spheres could exceed the number of inner spheres by a factor equal to the total number of images per conductor (which is typically near 20). Therefore, the number of outer spheres is the dominant factor in determining the total memory usage when a stratified dielectric medium is involved. It should be noted that, in the free-space case, the number of outer and inner spheres are identical, and that the introduction of a layered medium does not effect the number of required inner spheres. As will be shown in this section, the specific spatial arrangement of the image charges due to the stratified dielectric medium can be exploited to substantially reduce the number of outer spheres to be stored. This yields a more efficient, adaptive, fast-multipole-based algorithm, with memory requirements that “approach” those of the more efficient free-space algorithm. The new adaptive algorithm will be referred to as AFMM.

The use of the closed-form Green’s function leads to the presence of a finite number of images, as illustrated in Figure 1. The important point to note is that, in many cases, a vast majority of the cubes that contain only image charges

are far removed from the cubes containing genuine charges. This suggests that, once the computational domain including all image patches is recursively subdivided into cubes, there may be many cubes that contain only image patches and whose corresponding outer spheres are not used in the construction of any inner spheres. Such outer spheres only serve to construct the outer spheres of the corresponding parent cubes. This is illustrated schematically in Figure 2. The shaded bold circles represent outer spheres of cubes that contain only image patches and which are not used to construct any inner spheres. From here on, outer spheres that are required for creating inner spheres are termed useful.

The above-described FMM algorithm requires direct potential evaluation to construct the outer spheres for all nonempty cubes at the finest level, irrespective of whether these outer spheres are useful or not. The finest level outer spheres are then used to recursively construct outer spheres for the parent cubes. These outer spheres at coarser levels are constructed whether they are useful or not. The approach followed in AFMM is to bypass the construction of outer spheres that are not useful. This is achieved in a recursive manner, as follows. Every useful outer sphere is constructed by adding up two distinct types of contributions, as shown in Figure 3c. First, if any

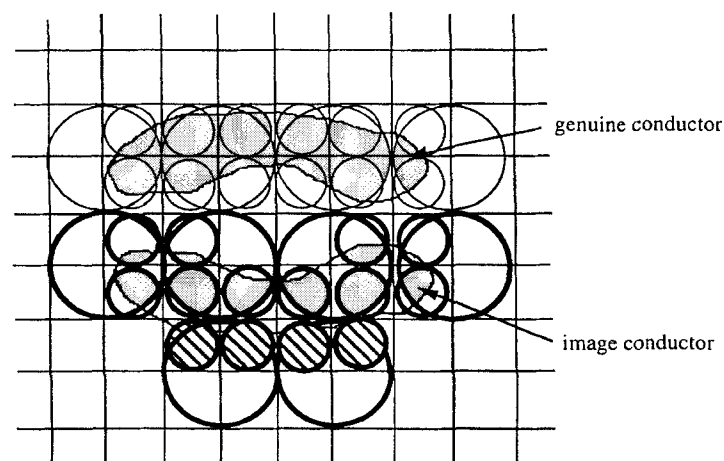


Figure 2. Configuration of a part of the computational domain, comprising of the genuine conductor and one image, as illustrated in the dashed box in Figure 1. A genuine conductor is present in the upper half of the square, and one of the images is shown in the lower half. Bold circles depict outer spheres for cubes containing image (source) patches only, while light circles depict inner spheres for cubes containing genuine (source and observation) patches. The shaded bold circles represent outer spheres that do not “interact” with the inner spheres. The FMM algorithm uses these outer spheres only for constructing larger outer spheres. AFMM bypasses the construction of these outer spheres to significantly reduce the memory requirements of the algorithm.

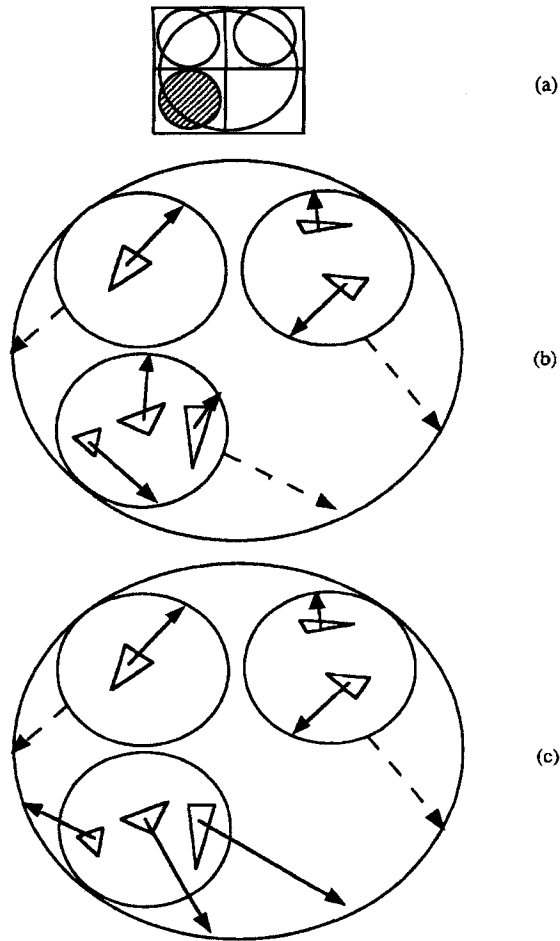


Figure 3. Construction of outer spheres in FMM and AFMM. (a) A typical configuration in the computational domain. An outer sphere and the corresponding child outer spheres are shown. The shaded circle represents an outer sphere that is not used to construct any inner sphere. (b) In FMM, the outer sphere for the parent cube is obtained by using the outer sphere formula (dashed arrows) and summing the contributions from each of spheres corresponding to the child cubes. (c) In AFMM, the outer sphere for the parent cube is constructed using the outer sphere formula (dashed arrows) from those child cubes that have outer spheres, and direct evaluation from the patches that reside in the cube whose outer sphere has not been constructed. The number of direct computations is the same in (b) and (c), whereas one extra outer sphere is computed, stored, and used in (b).

of the outer spheres corresponding to the child cubes are useful (and therefore exist), contributions from such spheres are utilized in exactly the same manner as in the FMM; i.e., by invoking the outer sphere formula [eq. (6)]. Second, the potentials due to patches in child cubes whose outer spheres are not useful (and therefore do not

exist) are evaluated directly on the surface of the useful outer sphere that is to be constructed. The recursion is initiated by using direct potential evaluation to construct useful outer spheres corresponding to those cubes whose descendants have no useful outer spheres. It is easily verified that the number of direct potential evaluations required in FMM and AFMM are the same; however, FMM typically constructs, stores, and uses many more outer spheres. Both techniques require the same number of inner spheres. As mentioned earlier, the major component of memory usage are the number of outer and inner spheres. The fact that, for frequently encountered structures, much fewer outer spheres need to be stored in AFMM renders it more memory efficient than FMM. The memory saving can be considerable, depending on the specific configuration of images. This is corroborated by the examples shown in the next section. The AFMM algorithm, when used in conjunction with an iterative solver such as GMRES, necessitates the identification of all required outer spheres prior to the start of the iterative process. This is achieved by performing one dry-run pass through the original FMM to mark the outer spheres that are called for during the construction of inner spheres. No actual potential computations need to be carried out during the dry-run, and therefore the computational overhead due to this dry-run is negligible.

An *a priori* estimate for the savings in the number of spheres to be stored can be derived for a model canonical problem. Consider a conducting plate, of side d , placed above a parallel infinite PEC at a distance of $d/2$. If h is the length of the side of a cube at the finest level L , and $d \approx O(2^{L-k}h)$, $k \in \{0, 1, \dots, L\}$, then the outer spheres that are actually utilized in AFMM while constructing inner spheres are those at level $k + 1$. In AFMM, there are $2^{2k+2} + 2^{2k+4} + \dots + 2^{2L}$ outer spheres for the plate and 2^{2k+2} outer spheres for the image. In FMM, the total number of outer spheres is $2(2^{2k+2} + 2^{2k+4} + \dots + 2^{2L})$. The number of inner spheres in both methods is $(2^{2k+2} + 2^{2k+4} + \dots + 2^{2L})$, constructed for the plate only. Hence, the relative memory saving with AFMM is

$$\frac{\left(\frac{\{2^{2(L-k)} - 1\}}{3} - 1 \right)}{2^{2(L-k)} - 1}.$$

This figure is for a single image; the number of images due to a stratified dielectric is much larger (around 20) and a larger memory saving is therefore expected for realistic problems. This leads to savings that are typically greater than 60%.

AFMM requires no more CPU time per iteration than FMM does. In both FMM and AFMM, most of the computation time is spent in the construction of inner spheres rather than outer spheres, and both algorithms require the construction of an identical number of inner spheres. Therefore, the fact that a smaller number of outer spheres are required in AFMM does not manifest itself in any significant reduction of CPU time.

AFMM produces as accurate capacitance matrix entries as the FMM. Inaccuracies in the FMM and AFMM arise when truncating the number of harmonics in the outer and inner sphere formulas, eqs. (4) and (5). Because AFMM constructs fewer outer spheres than FMM, one would expect less error propagation. However, provided that a sufficiently large number of harmonics is used in both the AFMM and the FMM, the two techniques produce nearly the same values.

In the best case, where FMM constructs no outer spheres that are not used in the construction of inner spheres, AFMM and FMM are identical. However, as mentioned earlier, when dealing with typical structures the vast majority of outer spheres are redundant, in which case the AFMM will require substantially less memory than the FMM without any adverse effects on CPU time or accuracy. The relatively simple modification suggested in this section has a tremendous impact on memory usage; on a given computer platform, AFMM can solve much larger problems than the FMM can.

4. NUMERICAL RESULTS

The above-described FMM and AFMM algorithms are used in conjunction with the GMRES iterative method, leading to two iterative solution techniques. To compare the memory requirements, CPU times, and accuracy of the adaptive algorithm (termed AFMM-GMRES) with that of the nonadaptive algorithm (termed FMM-GMRES), these two methods are employed to obtain the capacitance matrices of the structures shown in Figure 4, namely a conducting plate, an airbridge, a 10-conductor microstrip crossover, and a 4-conductor bus crossing, all embedded in a

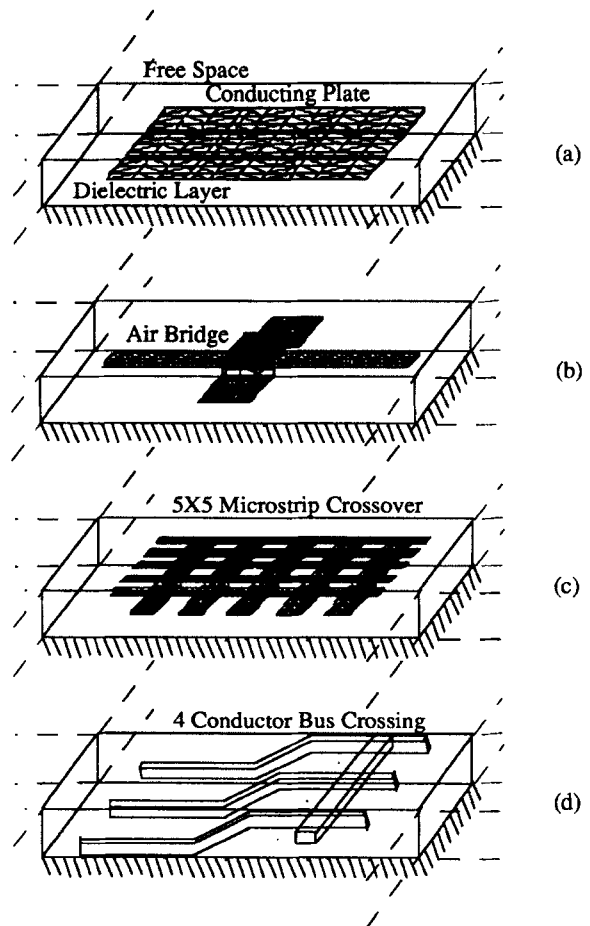


Figure 4. Structures to be used for testing the FMM-based capacitance computation algorithms. The structures are a conducting plate (a), an airbridge (b), a 10-conductor microstrip crossover (c), and a 4-conductor bus crossing, all embedded in a dielectric slab of infinite extent with thickness 5×10^{-3} m with a relative permittivity of 5. The dielectric is backed by an infinite ground plane.

dielectric of finite thickness which is backed by a ground plane.

Table I shows the number of outer and inner spheres required to be stored in FMM-GMRES and AFMM-GMRES. As mentioned in section 3, practically all the memory usage of these algorithms is due to storing outer spheres. In all cases, there is a substantial memory saving of at least 38% and, in many cases, it is much higher. As the number of cubes used in the fast-multipole algorithm is increased, the percentage memory saving achieved by using AFMM over FMM is increased, and is as high as 80% in one case. Another advantage of AFMM-GMRES is that a larger number of levels can be used in the fast

TABLE I. Memory Requirements of the Two Fast-Multipole-Based Methods

Problem	Total Number of Cubes	Number of Outer Spheres in FMM-GMRES	Number of Outer Spheres in AFMM-GMRES	Number of Inner Spheres	Percentage Saving in Memory (1%)
Plate	4681	2371	1372	234	38.3
-do-	37,449	5371	1396	434	68.5
-do-	299,593	8971	2172	634	70.8
Airbridge	4681	1256	628	136	45.1
-do-	37,449	6081	1972	484	62.6
-do-	299,593	24,721	3680	1632	79.8
5 × 5 microstrip crossover	4681	2204	1156	217	43.3
-do-	37,449	10,475	2776	865	67.9
-do-	299,593	25,254	4612	1782	76.4
4-conductor bus crossing	4681	1458	823	182	38.7

multipole algorithm without expending memory, thereby reducing the number of patches that are present in cubes that are not “well-separated” at the finest level. This in turn implies that the number of direct interactions to be computed is also reduced. Furthermore, as discussed in section 3, the number of outer spheres required in AFMM-GMRES, “approach” the number of inner spheres. Although the ratio of outer to inner spheres is still greater than 1, it is not close to the number of images which is the case with the less memory-efficient FMM-GMRES. The memory requirements of AFMM-GMRES are therefore closer to those of the free-space fast-multipole algorithm (where the number of outer and inner spheres is the same) than FMM-GMRES.

Table II shows a comparison of the CPU times required by the two methods for the different problems. A total of 4681 cubes (four levels) are used in the fast-multipole algorithms. AFMM-GMRES and FMM-GMRES require nearly the same CPU time in all the cases considered, as discussed in section 3. As shown in ref. 14, the

FMM-GMRES technique is itself much faster than the non-FMM-based direct or iterative methods.

The entries of the capacitance matrices obtained by FMM-GMRES and AFMM-GMRES are compared with those obtained by using the direct LU decomposition technique. A total of 4681 cubes (four levels) are used in the fast-multipole algorithms. Four harmonics are used in the outer and sphere formulas [eqs. (4) and (5)]. The error tolerance in GMRES is set to 10^{-3} . For the conducting plate, LU decomposition produced a capacitance value of 71.9 pF, while FMM-GMRES gave a value of 72.3 pF, and AFMM-GMRES yielded a value of 72.0 pF. For the airbridge, Table III shows that both the FMM-based techniques produced equally accurate results. The first row of the capacitance matrix for the 10-conductor microstrip crossover problem is shown in Table IV. All three techniques produced almost exactly the same values; the relative mean square errors for the entire capacitance matrix are 0.82% for FMM-GMRES and 0.78% for

TABLE II. CPU Times, on a DEC-Alpha, for Computing the Capacitance Matrices of the Structures Shown in Figure 4

Problem	Number of Conductors	Total Number of Patches	FMM-GMRES CPU Time (min)	AFMM-GMRES CPU Time (min)
Plate	1	4200	0.79	0.75
Airbridge	2	37,296	2.77	2.35
5 × 5 microstrip crossover	10	20,160	9.75	9.27
4-conductor bus crossing	4	78,624	11.91	11.61

TABLE III. Capacitance Matrix Entries of the Dielectric-Embedded Airbridge

Matrix Entry	LU (pF)	FMM-GMRES (pF)	AFMM-GMRES (pF)
C_{11}	30.78	30.81	30.81
C_{12}	-2.19	-2.15	-2.15
C_{22}	40.20	40.19	40.19

AFMM-GMRES. The entries of the capacitance matrix for the four conductor bus crossing is shown in Table V. Again, the three methods produced nearly identical results; the relative mean square errors for the capacitance matrix are 0.50% for FMM-GMRES and 0.48% for AFMM-GMRES.

5. CONCLUSIONS AND SCOPE FOR FUTURE WORK

In this article, the adaptive AFMM algorithm for the capacitance computation of structures embedded in a stratified medium has been introduced, and a study comparing the memory usage, CPU time requirements, and the accuracies of the AFMM and the nonadaptive FMM algorithms has been carried out. The memory requirements of both the FMM and AFMM algorithms are essentially determined by the number of outer and inner spheres that need to be stored. For typical structures, FMM requires a much greater number of outer spheres than inner spheres. It is shown that, for those structures, AFMM requires far fewer outer spheres than FMM, which results in large savings in overall

TABLE IV. First Row of the Capacitance Matrix for the Dielectric-Embedded Microstrip

Matrix Entry	Value (pF)
C_{11}	20.9
C_{21}	-0.1
C_{31}	0.0
C_{41}	0.0
C_{51}	0.0
C_{61}	-0.6
C_{71}	-0.6
C_{81}	-0.6
C_{91}	-0.6
$C_{10,1}$	-0.6

TABLE V. Capacitance Matrix for the 4-Conductor Bus Crossing (Element Values in pF)

13.0	-0.1	0.0	-0.9
-0.1	13.0	-0.1	-1.1
0.0	-0.1	13.0	-0.9
-0.9	-1.1	-0.9	16.0

memory requirements. In terms of the number of outer spheres required for computations involving structures in layered dielectric media, AFMM is much closer to the efficient free-space algorithm than to its stratified media FMM predecessor. These memory savings are dependent on the number of levels used in the fast-multipole algorithm. As more levels are used, the relative memory saving achieved by using AFMM over FMM increases, and it was observed to be as high as 80% in one case in which 299,593 cubes (six levels) were employed. The reduced memory requirement of the AFMM algorithm enables one to tackle larger problems on a given computer platform than is possible by using the FMM algorithm. AFMM also requires no more CPU time and produces as accurate results as does the FMM algorithm.

The results presented in this article are for a single dielectric layer. However, the technique discussed both herein, and in ref. 14 can be readily extended to the multilayer case, and this extension is currently being implemented.

ACKNOWLEDGMENT

The authors thank the anonymous reviewers for their useful comments.

REFERENCES

1. K. S. Oh, D. Kuznetsov, and J. E. Schutt-Aine, "Capacitance Computations in a Multilayered Dielectric Medium Using Closed-Form Spatial Green's Functions," *IEEE Trans. Microwave Theory Tech.*, Vol. 42, Aug. 1994, pp. 1443-1453.
2. L. Greengard and V. Rokhlin, "A Fast Algorithm for Particle Simulations," *J. Comp. Phys.*, Vol. 73, 1987, pp. 325-348.
3. L. Greengard, *The Rapid Evaluation of Potential Fields in Particle Systems*. Cambridge, MA: MIT Press, 1988.

4. V. Rokhlin, "Rapid Solution of Integral Equations of Classical Potential Theory," *J. Comp. Phys.*, Vol. 60, Sept. 1985, pp. 187–207.
5. J. Carrier, L. Greengard, and V. Rokhlin, "A Fast Adaptive Multipole Algorithm for Particle Simulations," *SIAM J. Sci. Statist. Comput.*, Vol. 9, July 1988, pp. 669–686.
6. C. R. Anderson, "An Implementation of the Fast Multipole Method Without Multipoles," *SIAM J. Sci. Statist. Comput.*, Vol. 13, July 1992, pp. 923–947.
7. K. Nabors and J. White, "A Fast Multipole Algorithm for Capacitance Extraction of Complex 3-d Geometries," in *Proceedings of the IEEE Custom Integrated Circuits Conference*. San Francisco: IEEE Press, 1989.
8. K. Nabors, S. Kim, J. White, and S. Senturia, "Fast Capacitance Extraction of General Three-Dimensional Structures," in *Proceedings of the 1991 IEEE International Conference on Computer Design: VLSI in Computers and Processors*, Oct. 1991, pp. 479–484.
9. K. Nabors and J. White, "FastCap: a multipole accelerated 3-d capacitance extraction program," *IEEE Trans. CAD*, Vol. 10, Nov. 1991, pp. 1447–1459.
10. K. Nabors, S. Kim, and J. White, "Fast Capacitance Extraction of General Three-Dimensional Structures," *IEEE Trans. Microwave Theory Tech.*, Vol. 40, July 1992, pp. 1496–1506.
11. K. Nabors and J. White, "Multipole-Accelerated Capacitance Extraction Algorithms for 3-d Structures with Multiple Dielectrics," *IEEE Trans. Circ. Syst.—I*, Vol. 39, Nov. 1992.
12. K. Nabors and J. White, "Multipole-Accelerated 3-d Capacitance Extraction Algorithms for Structures with Conformal Dielectrics," *29th ACM/IEEE Design Automation Conference*, 1992.
13. S. Rao, T. Sarkar, and R. Harrington, "The Electrostatic Field of Conducting Bodies in Multiple Dielectric Media," *IEEE Trans. Microwave Theory Tech.*, Vol. 32, Nov. 1984, pp. 1441–1448.
14. V. Jandhyala, E. Michielssen, and R. Mittra, "Multiple-Accelerated Capacitance Computation for 3-d Structures in a Stratified Dielectric Medium Using a Closed-Form Green's Function," *Int. J. MIMI-CAE*, Vol. 5, March 1995, pp. 68–78.
15. V. Jandhyala, E. Michielssen, and R. Mittra, "Fast Capacitance Computations for Conducting Structures Embedded in a Multilayered Dielectric Medium Using the Fast Multipole Algorithm and a Closed Form Green's Function," presented at the 3rd Topical Meeting on Electrical Performance of Electronic Packaging, Nov. 1994.
16. R. F. Harrington, *Field Computation by Moment Methods*. Malabar, FL: Krieger, 1982.
17. Y. Saad and M. H. Schultz, "GMRES: a generalized minimal residual algorithm for solving non-symmetric linear systems," *SIAM J. Sci. Statist. Comput.*, Vol. 7, July 1986, pp. 856–869.
18. G. Golub and C. Van Loan, *Matrix Computations*. Baltimore, MD: Johns Hopkins University Press, 1983.
19. A. H. Stroud, *Approximate Calculation of Multiple Integrals*. Englewood Cliffs, NJ: Prentice-Hall, 1971.
20. A. D. McLaren, "Optimal Numerical Integration on a Sphere," *Math. Comput.*, Vol. 17, 1963, pp. 361–383.

BIOGRAPHIES



Vikram Jandhyala was born on January 4, 1972, in New Delhi, India. He received the BTech degree in electrical engineering from the Indian Institute of Technology, Delhi, in 1993, and the MS degree in electrical engineering from the University of Illinois at Urbana-Champaign, in 1995. He is currently pursuing his PhD in the Department of Electrical and Computer Engineering at the University of Illinois, Urbana-Champaign. From 1993 to 1995, he was a graduate research assistant in the Electromagnetics Communication Laboratory at the University of Illinois. Presently, he is a graduate research assistant in the Center for Computational Electromagnetics at the University of Illinois. His current research is in the area of fast algorithms for electromagnetic scattering and high-speed circuits. Mr. Jandhyala is a member of Phi Kappa Phi and a student member of the IEEE.



Eric Michielssen (MS in electrical engineering Katholieke Universiteit Leuven [KUL], Belgium, 1987; PhD University of Illinois at Urbana-Champaign, 1992) is assistant professor of electrical and computer engineering at the University of Illinois at Urbana-Champaign and associate director of its Center for Computational Electromagnetics. From 1987 to 1988, he was a research assistant in the Microwaves and Lasers Laboratory at KUL. In 1988, he was appointed Belgian American Educational Foundation Fellow. He joined the faculty of the Department of Electrical and Computer Engineering at the University of Illinois as a visiting assistant professor in 1992, and was appointed assistant professor of electrical and computer engineering in 1993. He is a 1995 NSF Career Award recipient. His research interests include all aspects of computational electromagnetics with a focus on fast multilevel algorithms, the application of combinatorial stochastic optimization techniques to the design of electromagnetic and optical components, and computational photonics.



Raj Mittra is the director of the Electromagnetic Communication Laboratory of the Electrical and Computer Engineering Department and research professor of the Coordinated Science Laboratory at the University of Illinois. He is a fellow of the IEEE (Institute of Electrical and Electronical Engineers), a past-president of IEEE-AP-S (Antennas and Propagation Society), and he has served as the editor of *Transactions of the Antennas and Propagation Society*. He won the Guggenheim Fellowship Award in 1965 and the IEEE Centennial Medal in 1984. He has been a visiting professor at Oxford

University, Oxford, England, and at the Technical University of Denmark, Lyngby, Denmark. Currently, he serves as the North American editor of the journal, *AEÜ*. He is president of RM Associates, which is a consulting organization providing services to several industrial and governmental organizations. His professional interests include the areas of electromagnetic modeling and simulation of electronic packages, communication antenna design including GPS, broadband antennas, EMC analysis, radar scattering, frequency-selective surfaces, microwave and millimeter-wave integrated circuits, and satellite antennas. He has published approximately 400 journal papers and 20 books or book chapters on various topics related to electromagnetics.